N93-19394

1992 NASA/ASEE SUMMER FACULTY FELLOWSHIP PROGRAM

JOHN F. KENNEDY SPACE CENTER
UNIVERSITY OF CENTRAL FLORIDA

CALIBRATION OF THE ARID ROBOT

PREPARED BY:	Dr. Keith L. Doty
ACADEMIC RANK:	Professor
UNIVERSITY AND DEPARTMENT:	University of Florida Department of Electrical Engineering
NASA/KSC	
DIVISION:	Mechanical Engineering Directorate
BRANCH:	Special Projects (RADL)
NASA COLLEAGUE:	Willis Crumpler Bill Jones Eduardo Lopez
DATE:	August 7, 1992
CONTRACT NUMBER:	University of Central Florida NASA-NGT-60002 Supplement: 8

ACKNOWLEDGEMENTS

The author gratefully acknowledges the support of the University of Central Florida faculty and staff along with the Boeing and NASA staffs whose diligence and kindness make the NASA Faculty Fellowship program at the Kennedy Space Center so efficient and productive. Particular thanks to Willis Crumpler, Bill Jones, Eduardo Lopez, Gabor Tamasi, Todd Graham and Carol Valdez of NASA; Ron Remus, Joe Looney, Jose Lago and Brian Yamauchi of Boeing and Loren Anderson and Kari Stiles of the University of Central Florida. A special thanks to my office mate, Carl Latino of Oklahoma State University, for stimulating discussions and all-around good fellowship.

ABSTRACT

The author has formulated a new, general model for specifying the kinematic properties of serial manipulators. The new model kinematic parameters do not suffer discontinuities when nominally parallel adjacent axes deviate from exact parallelism. From this new theory the author develops a first-order, lumped-parameter, *calibration-model* for the ARID manipulator. Next, the author develops a calibration methodology for the ARID based on visual and acoustic sensing. A sensor platform, consisting of a camera and four sonars attached to the ARID end frame, performs calibration measurements. A calibration measurement consists of processing one visual frame of an accurately placed calibration image and recording four acoustic range measurements. A minimum of two measurement protocols determine the kinematics calibration-model of the ARID for a particular region: assuming the joint displacements are accurately measured, the calibration surface is planar, and the kinematic parameters do not vary rapidly in the region. No theoretical or practical limitations appear to contra-indicate the feasibility of the calibration method developed here.

TABLE OF CONTENTS

1.0 PROJECT DESCRIPTION

Parameter and assembly tolerances and non-rigid-body effects due to link and joint flexion and thermal expansion introduce errors into the tool pose at the end-effector of a robot. Accounting for the various sources of kinematic error by means of a lumped, first-order model allows one to compensate for pose errors at different configurations. By calibrating the robot at discrete poses, designated *calibration poses* , in the region of its workspace where it will see service, one increases the robot's overall accuracy at those poses. The error-model will then permit interpolation between calibration poses to increase the accuracy of the robot at non-calibration poses.

The primary goal of this project is to increase the operational accuracy of the ARID robot through calibration and adjustments in the ARID control software.

Success in calibration hinges on the performance of the the following tasks,

1. Develop an appropriate kinematics model of the ARID robot to account for the observed end-frame positioning errors.
2. Identify a measurement technique for accurately determining the poses of the ARID robot.
3. Determine the critical calibration poses for measurement.
4. Measure ARID positioning errors at the critical calibration poses..
5. Develop, interface and test a computer program that will use experimentally measured data to compensate for ARID's inaccuracies.

Points 4 and 5 are not addressed in this paper.

2.0 SUMMARY OF PROGRESS

During this program the author has

1. Formulated a kinematics model for calibration,
2. Developed a calibration methodology for the ARID
3. Measured the angular error about the x- and y-*axes* of the ARID end-frame for a variety of configurations. This effort is given in another report [1].

Work yet to be done,

1. Complete the derivation of the ARID calibration-model and devise a methodology for solving for the error parameters.
2. Configure the Perceptics NuVision system and write C-code to perform the required blob analysis on the proposed calibration square.
3. Design and configure a calibration sensor-platform consisting of a camera and four sonar sensors.
4. Write software to acquire visual and acoustic data from the sensor platform.
5. Implement the calibration algorithms in software.
6. Test the calibration sensor-platform on a calibration square lying on a microscopically flat table.
7. Compute the ARID calibration model from calibration measurements.
8. Test and verify the derived calibration model.

In the next section, the author develops a general calibration model with general applicability.

3. KINEMATICS MODEL FOR CALIBRATION

A lumped kinematics model for calibration has been devised. The lumped-parameter calibration model is given in Table 3.1. The parameters found in the table are defined in Fig. 3.1. This model's parameters do not depend on the common normal between two axes, hence, the calibration parameters do not suffer the discontinuities incurred by the Denavit-Hartenburg parameters with nominally parallel axes.

Table 3.1 : Calibration Kinematic Parameters for the ARID Robot

Joint	d	θ	β	a	α	Joint Limits
1 p	d_1	θ_1	β_1	a_1	α_1	[0*inches*, 718*inches*]
2 r	0	θ_2	β_2	a_2	α_2	[4° , 112°]
3 r	0	θ_3	β_3	a_3	α_3	[102° , 148°]
4 r	0	θ_4	0°	0	0°	[-16° , -117°]

The angle parameters θ, β, α, will be called the *joint-angle, link pitch and link twist* , respectively. The parameter d is the *link offset* and a the *link length* . These parameters are determined as follows.

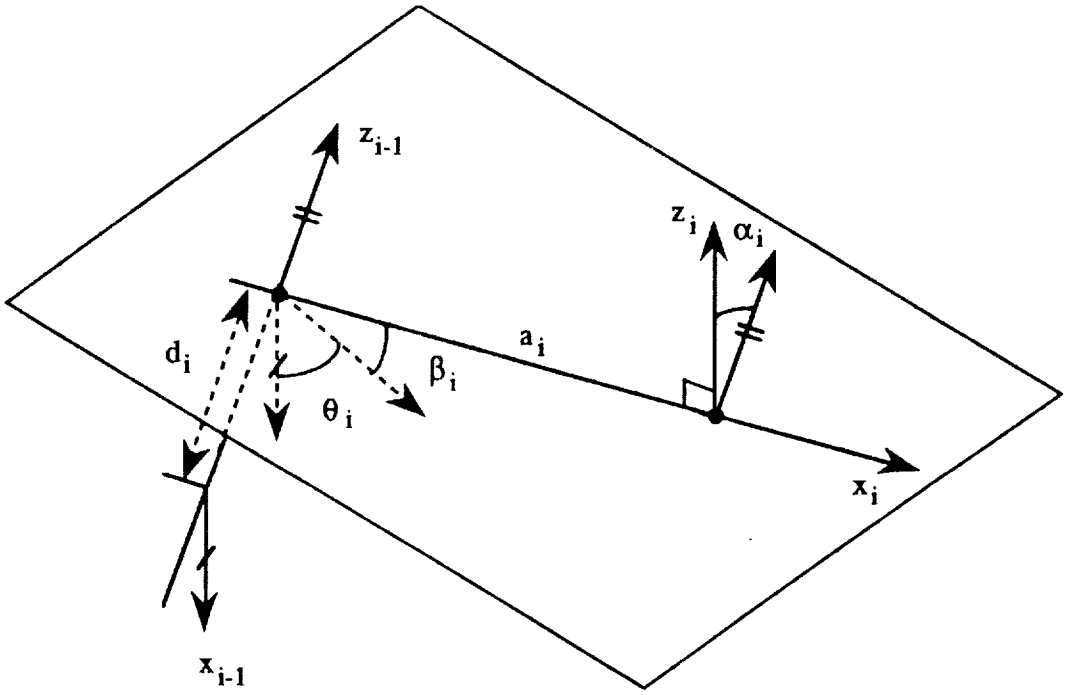

Figure 3.1 Calibration-model kinematic parameters between adjacent joint axes of a serial manipulator.

Draw a perpendicular line from the origin of frame F_{i-1} to the z_i *-axis* with $d_i = 0$. The intersection of this perpendicular line with the z_i *-axis* defines the origin of the next link frame, F_i . The length of this perpendicular line equals a_i . For revolute joints d_i always equals zero. For prismatic joints, d_i equals the joint displacement. Thus, for revolute joints, this model has the same number of parameters as the DH-model, namely, four. With prismatic joints, however, this model requires a fifth parameter, the link offset d_i .

The angle θ equals the amount of rotation about the z_{i-1} *-axis* required to make the z_{i-1} *-axis* , the x_{i-1} *-axis* and the line a_i coplanar. Rotating β_i about the new *y-axis* aligns the new *x-axis* to the line a_i . Translation along the line a_i moves the frame to the origin of F_i . To finish the alignment, twist the moving frame *z-axis* about the line a_i by the angle α_i to align it with the z_i *-axis* .

In summary, the sequence of coordinate transformations between successive joint frames to generate the link transformation $\mathbf{L}_i$ consists of the following:

Revolute Joint:

$$\mathbf{L}_i := \text{Rotate}(z, \theta_i)\ \text{Rotate}(y, \beta_i)\ \text{Translate}(x, a_i)\ \text{Rotate}(x, \alpha_i)$$

Prismatic Joint:

$$\mathbf{L}_i := \text{Translate}(z, d_i)\ \text{Rotate}(z, \theta_i)\ \text{Rotate}(y, \beta_i)\ \text{Translate}(x, a_i)\ \text{Rotate}(x, \alpha_i)$$

The link transform, therefore, computes to

$$\mathbf{L}_i := \begin{bmatrix} \mathbf{R}_i & \mathbf{l}_i \\ 0\ 0\ 0 & 1 \end{bmatrix}, \tag{3-1}$$

where

$$\mathbf{R}_i = \begin{bmatrix} c_{\beta i}\, c_{\theta i} & c_{\theta i}\, s_{\alpha i}\, s_{\beta i} - c_{\alpha i}\, s_{\theta i} & c_{\alpha i}\, c_{\theta i}\, s_{\beta i} + s_{\alpha i}\, s_{\theta i} \\ c_{\beta i}\, s_{\theta i} & c_{\alpha i}\, c_{\theta i} + s_{\alpha i}\, s_{\beta i}\, s_{\theta i} & -c_{\theta i}\, s_{\alpha i} + c_{\alpha i}\, s_{\beta i}\, s_{\theta i} \\ -s_{\beta i} & c_{\beta i}\, s_{\alpha i} & c_{\alpha i}\, c_{\beta i} \end{bmatrix} \tag{3-2}$$

and

$$\mathbf{l}_i := \begin{bmatrix} a_i\, c_{\beta i}\, c_{\theta i} \\ a_i\, c_{\beta i}\, s_{\theta i} \\ d_i - a_i\, s_{\beta i} \end{bmatrix} \tag{3-3}$$

The full forward kinematics ${}^0\mathbf{T}_4$ for the ARID equals

$${}^0\mathbf{T}_4 = \mathbf{L}_1\, \mathbf{L}_2\, \mathbf{L}_3\, \mathbf{L}_4\,. \tag{3-4}$$

Symbolic computation of the complete expression for ${}^0\mathbf{T}_4$ probably exceeds practical requirements. Since each link twist α_i and link pitch β_i lie close to zero, second-order and higher terms in these variables may be ignored. ${}^0\mathbf{T}_4$ will be computed only to first order terms in the α_i and β_i . This computation

appears in Section 3.2. Before continuing further, it will be instructive to define the various coordinate frames involved in this report.

3.1 Identifying the Various Coordinate Frames

Figure 3.2 indicates the relative orientation of the principle coordinate frames discussed in this report. The camera frame is defined at the lens center and the image frame on the image plane. Each calibration square on the calibration strip defines a calibration frame. The ARID base frame follows from the standard link frame definitions. Motion along the ARID base frame *z-axis* , therefore, corresponds to moving along the Orbiter's *x-axis*. To simplify the ensuing discussions, the term *ARID* in this report refers to the ARID on the Orbiter's starboard side.

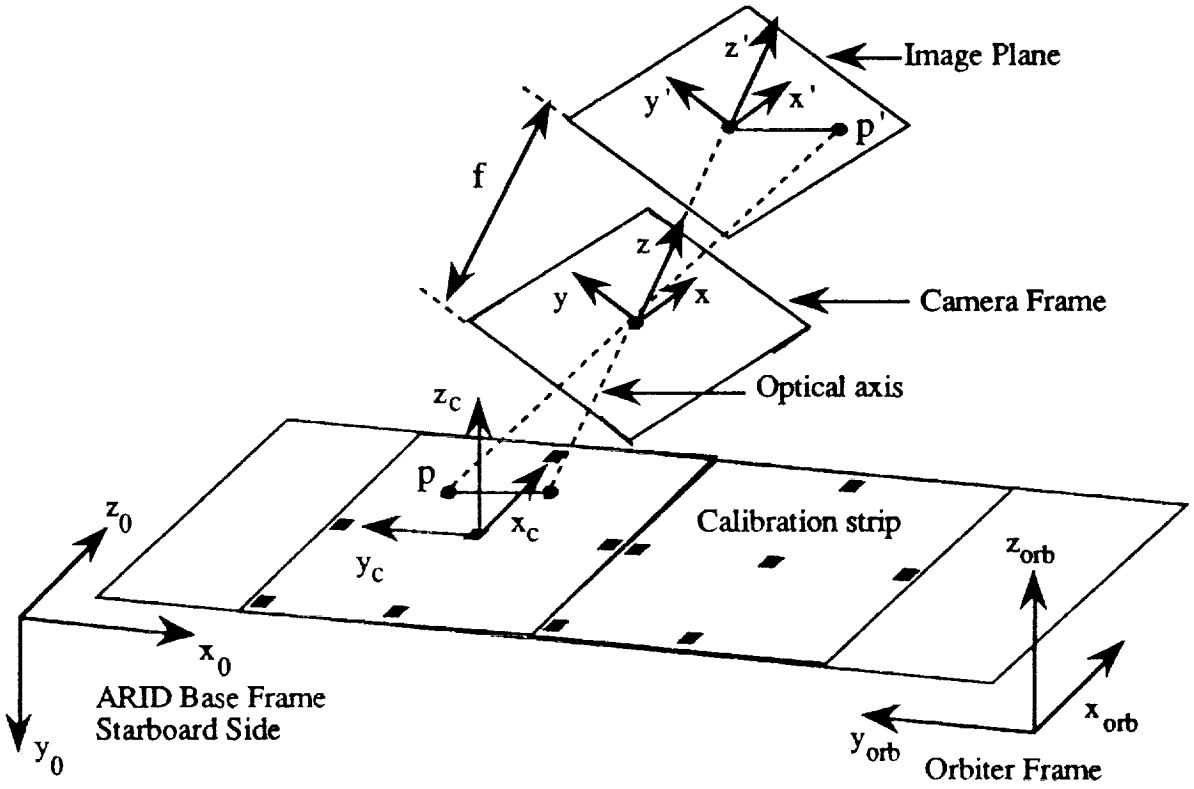

Figure 3.2 Depiction of the image, camera, calibration, ARID and Orbiter frames.

From Fig. 3.2 one determines that the rotation ${}^0\mathbf{R}_{orbiter}$,

$$ {}^{0}\mathbf{R}_{orbiter} = \begin{bmatrix} 0 & -1 & 0 \\ 0 & 0 & -1 \\ 1 & 0 & 0 \end{bmatrix}, $$

transforms Orbiter coordinates into Starboard-ARID base frame coordinates.

3.2 First-Order Calibration Model for the ARID

For manipulators where adjacent joint axes are nominally parallel, the link parameters α_i and β_i will be approximately zero. To first order,

$s_{\beta i} := \sin(\beta_i) \approx \beta_i$, $s_{\alpha i} := \sin(\alpha_i) \approx \alpha_i$, $c_{\beta i} := \cos(\beta_i) \approx 1$, $c_{\alpha i} := \cos\alpha_i) \approx 1$,

and $s_{\alpha i}\, s_{\beta i} \approx 0$. With these approximations the link transform rotation becomes

$$ \mathbf{R}_i = \begin{bmatrix} c_{\theta i} & -s_{\theta i} & \beta_i c_{\theta i} + \alpha_i s_{\theta i} \\ s_{\theta i} & c_{\theta i} & -\alpha_i c_{\theta i} + \beta_i s_{\theta i} \\ -\beta_i & \alpha_i & 1 \end{bmatrix} \qquad (3\text{-}5) $$

and

$$ \mathbf{l}_i := \begin{bmatrix} a_i c_{\theta i} \\ a_i s_{\theta i} \\ d_i - \beta_i a_i \end{bmatrix} \qquad (3\text{-}6) $$

Suppose links one and two have nominally parallel joint axes, then the first-order approximation of

$$ \mathbf{L}_1 \mathbf{L}_2 = \begin{bmatrix} \mathbf{R}_1 \mathbf{R}_2 & \mathbf{R}_1 \mathbf{l}_2 + \mathbf{l}_1 \\ 0\ 0\ 0 & 1 \end{bmatrix}, \qquad (3\text{-}7) $$

consists of

$\mathbf{R}_1 \mathbf{R}_2 =$

$$\begin{bmatrix} c_{12} & -s_{12} & \beta_2 c_{12}+\alpha_2 s_{12}+\beta_1 c_1+\alpha_1 s_1 \\ s_{12} & c_{12} & \beta_2 s_{12}-\alpha_2 c_{12}+\beta_1 s_1-\alpha_1 c_1 \\ -\beta_1 c_2+\alpha_1 s_2-\beta_2 & \beta_1 s_2+\alpha_1 c_2+\alpha_2 & 1 \end{bmatrix} \quad (3\text{-}8)$$

and

$$\mathbf{R}_1 \mathbf{l}_2 + \mathbf{l}_1 = \begin{bmatrix} a_2 c_{12} + a_1 c_1 + d_2(\beta_1 c_1+\alpha_1 s_1) \\ a_2 s_{12} + a_1 s_1 + d_2(\beta_1 s_1-\alpha_1 c_1) \\ d_1 + d_2 + a_2(-\beta_1 c_2+\alpha_1 s_2-\beta_2) - \beta_1 a_1 \end{bmatrix} \quad (3\text{-}9)$$

Since the joint axes of the ARID are all nominally parallel, its first order calibration model may be computed using the general results in (3-8) and (3-9) to assist in the calculation of ${}^0\mathbf{T}_4 = \mathbf{L}_1 \mathbf{L}_2 \mathbf{L}_3 \mathbf{L}_4$. The results equal

$${}^0\mathbf{T}_4 = \begin{bmatrix} c_{1234} & -s_{1234} & \varepsilon_1 & a_1 c_1 + a_2 c_{12} + a_3 c_{123} \\ s_{1234} & c_{1234} & \varepsilon_2 & a_1 s_1 + a_2 s_{12} + a_3 s_{123} \\ \varepsilon_3 & \varepsilon_4 & 1 & d_1 + \varepsilon_5 \\ 0 & 0 & 0 & 1 \end{bmatrix} \quad (3\text{-}10)$$

where the first-order error terms $\varepsilon_1, \varepsilon_2, \varepsilon_3, \varepsilon_4, \varepsilon_5$ are given by

$$\varepsilon_1 = \beta_4 c_{1234} + \alpha_4 s_{1234} + \beta_3 c_{123} + \alpha_3 s_{123} + \beta_2 c_{12} + \alpha_2 s_{12} + \beta_1 c_1 + \alpha_1 s_1 \quad (3\text{-}11a)$$

$$\varepsilon_2 = \beta_4 s_{1234} - \alpha_4 c_{1234} + \beta_3 s_{123} - \alpha_3 c_{123} + \beta_2 s_{12} - \alpha_2 c_{12} + \beta_1 s_1 - \alpha_1 c_1 \quad (3\text{-}11b)$$

$$\varepsilon_3 = -\beta_1 c_{234} + \alpha_1 s_{234} - \beta_2 c_{34} + \alpha_2 s_{34} - \beta_3 c_4 + \alpha_3 s_4 - \beta_4 \quad (3\text{-}11c)$$

$$\varepsilon_4 = \beta_1 s_{234} + \alpha_1 c_{234} + \beta_2 s_{34} + \alpha_2 c_{34} + \beta_3 s_4 + \alpha_3 c_4 + \alpha_4 \quad (3\text{-}11d)$$

$$\varepsilon_5 = d_1 + a_3(-\beta_1 c_{23} + \alpha_1 s_{23} - \beta_2 c_3 + \alpha_2 s_3 - \beta_3) + a_2(-\beta_1 c_2 + \alpha_1 s_2 - \beta_2) - \beta_1 a_1 \quad (3\text{-}11e)$$

Equation (3-11) may be written more succinctly,

$$\varepsilon = \mathbf{E}\,\psi\,, \tag{3-12}$$

where

$$\varepsilon := [\varepsilon_1\ \varepsilon_2\ \varepsilon_3\ \varepsilon_4\ \varepsilon_5 - d_1]^\tau\,, \qquad \psi := [\beta_1\ \beta_2\ \beta_3\ \beta_4\ \alpha_1\ \alpha_2\ \alpha_3\ \alpha_4\ ]^\tau\,,$$

and

$\mathbf{E} =$

$$\begin{vmatrix} c_{1234} & c_{123} & c_{12} & c_1 & s_{1234} & s_{123} & s_{12} & s_1 \\ s_{1234} & s_{123} & s_{12} & s_1 & -c_{1234} & -c_{123} & -c_{12} & -c_1 \\ -c_{234} & -c_{34} & -c_4 & -1 & s_{234} & s_{34} & s_4 & 0 \\ s_{234} & s_{34} & s_4 & 0 & c_{234} & c_{34} & c_4 & 1 \\ -a_1 - a_2c_2 - a_3c_{23} & -a_2 - a_3c_3 & -a_3 & 0 & a_2s_2 + a_3s_{23} & a_3\,s_3 & 0 & 0 \end{vmatrix}$$

Observe that **E** only depends upon the joint angles θ_i and the link lengths a_i.

3.3 Solving for the ARID Kinematic Parameters

Let ${}^0\mathbf{M}_4$ be a measurement of the ARID end-frame pose expressed in the base frame. The calibration problem is to solve for the unknown kinematic parameters in ${}^0\mathbf{T}_4$ of (3-10), given one or more measurements: ${}^0\mathbf{M}_4 = {}^0\mathbf{T}_4$. At this juncture one must determine which kinematic parameters are known. For example, if d_1, the link lengths a_i , and the joint angles θ_i are known with a high degree of precision, one need only solve for ψ in (3-12). Since ψ contains eight unknowns, the system is under-determined for one measurement and over-determined with two measurements, assuming of course, that the β_i and α_i do not change significantly for the two robot configurations in which the measurements are made.

If all the kinematic parameters are unknown, the problem becomes non-linear. One can use the inverse kinematics solutions to express the *sines* and *cosines* of the revolute joint angles in terms of rational polynomials in the link lengths. The last column in ${}^0\mathbf{M}_4 = {}^0\mathbf{T}_4$ will then provide two equations in the three unknowns,

a_1, a_2, and a_3. Two measurements will yield four equations in the three link lengths. A least-squares solution can be employed to solve for them. With the link lengths determined, the joint angles for the two measurements may be calculated. Finally, one may compute ψ , given that d_1 has been calibrated separately. This procedure requires that the kinematic parameters do not vary significantly for the two measurement configurations of the robot.

The rest of this paper deals with how to generate the measurement poses ${}^0\mathbf{M}_4$.

4. Calibration Measurement Technique

The approach proposed here is to mount a digital camera and four sonic sensors onto the end-effector flange of the ARID robot with approximately the same total mass as the Lockheed end-effector. Refer to Figure 6.1 for a stylized side view of this calibration end-effector.

The camera pose with respect to the flange must be known. The camera will view a calibrated strip (Fig. 5.2) of four-inch squares with appropriate fiducial markings (Fig. 5.1). The calibration strip will run along the Orbiter *y-axis* on a partial, bay-door mock-up (Fig. 5.3). The strip permits a visual calibration measurement every four inches for a total of 28 measurements along the bay door. For high curvature areas of the bay-door, calibration might be required every one or two inches, particularly near the hinges. The author does not expect more than two or three such one-inch squares will be needed. Most calibration squares will be 4 inch squares. The number of calibration strips required will have to be determined by experiment.

A frame-grabber will be needed to capture the image and simple vision software to compute the gray level centroid for each fiducial mark. From these centroids the camera *x-y* position and orientation with respect to the image can be computed.

The four sonar sensors, arranged in an + pattern about the camera, compute the pitch and yaw of the camera frame and range data provides the distance from the camera center to the image center.

The sonar and vision measurements yield a total of six parameters and uniquely determines the pose of the camera, hence, the end-effector flange frame.

5. Vision Measurement

5.1 Details of the Calibration Square

Figure 5.1 illustrates one proposed calibration square. Each square contains five, solid fiducial squares $\frac{1}{4}" \times \frac{1}{4}"$ and a center fiducial $\frac{1}{2}" \times \frac{1}{4}"$. The centroids of these fiducial marks constitutes the critical information proffered by the calibration square. The fiducial in the upper left-hand-corner of the calibration square uniquely identifies quadrant two. Unless the robot end-effector pose deviates more than several inches, this fiducial mark will provide redundant information.

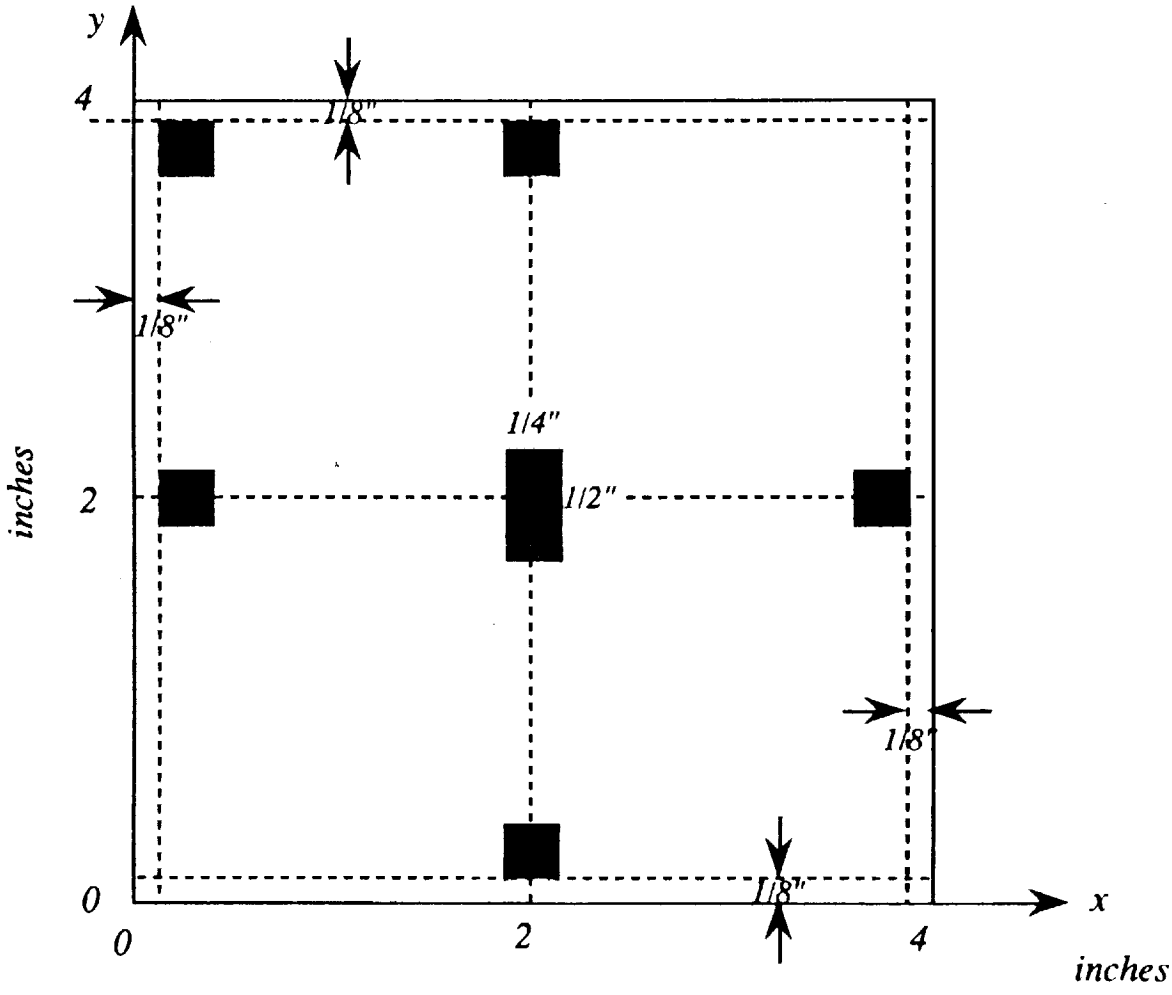

Figure 5.1 Typical visual calibration square.

The centroids of the remaining four perimeter fiducials determine the orientation and center of the calibration square with respect to the camera image. The upper-

center and lower-center fiducial centroids determine the vertical axis of the calibration square while the left-center and right-center fiducial centroids determine the horizontal axis of the calibration square. The centroid of the center fiducial marks the center of the calibration square and should be at the intersection of the vertical and horizontal axes determined by the other four just mentioned. The *y-axis* parallels the long side of the center fiducial and the *x-axis* parallels the short side.

The center fiducial, having twice the area of the other fiducials will be easy to identify in a camera image. From the center fiducial one can easily identify the others. In theory, the central fiducial yields all the information about the position and orientation of the calibration square. The redundant fiducials provided on the calibration square increase the the accuracy of the measurement.

Since the measurement of a fiducial centroid depends upon an area measurement, the computation will be robust to noise. Isolated white pixels in a black fiducial square will not significantly affect the computation of the fiducial's centroid.

For a 512×512 pixel camera, if the calibration frame fills the field of view, each pixel will correspond to a displacement of $\frac{4 \text{ inches}}{512} = \frac{1}{128}$ inch ≈ 0.0078 inches.

5.2 The Calibration Strip

A calibration strip consists of a sequence of concatenated calibration squares drawn on vellum or some other durable, thin, compliant material (Fig. 5.2). This strip, placed upon a mock-up segment of the bay door surface (Fig. 5.3) will permit visual calibration of the ARID robot at prescribed intervals. For instance, the ~112" width of the orbiter bay door divides into 28 four inch intervals. A calibration strip would consist of 28, four-inch squares. At the hinge-end of the bay door the sharp curvature over four inches may require adjustments to the sonar range measurement. This will be discussed in the section on sonar measurements.

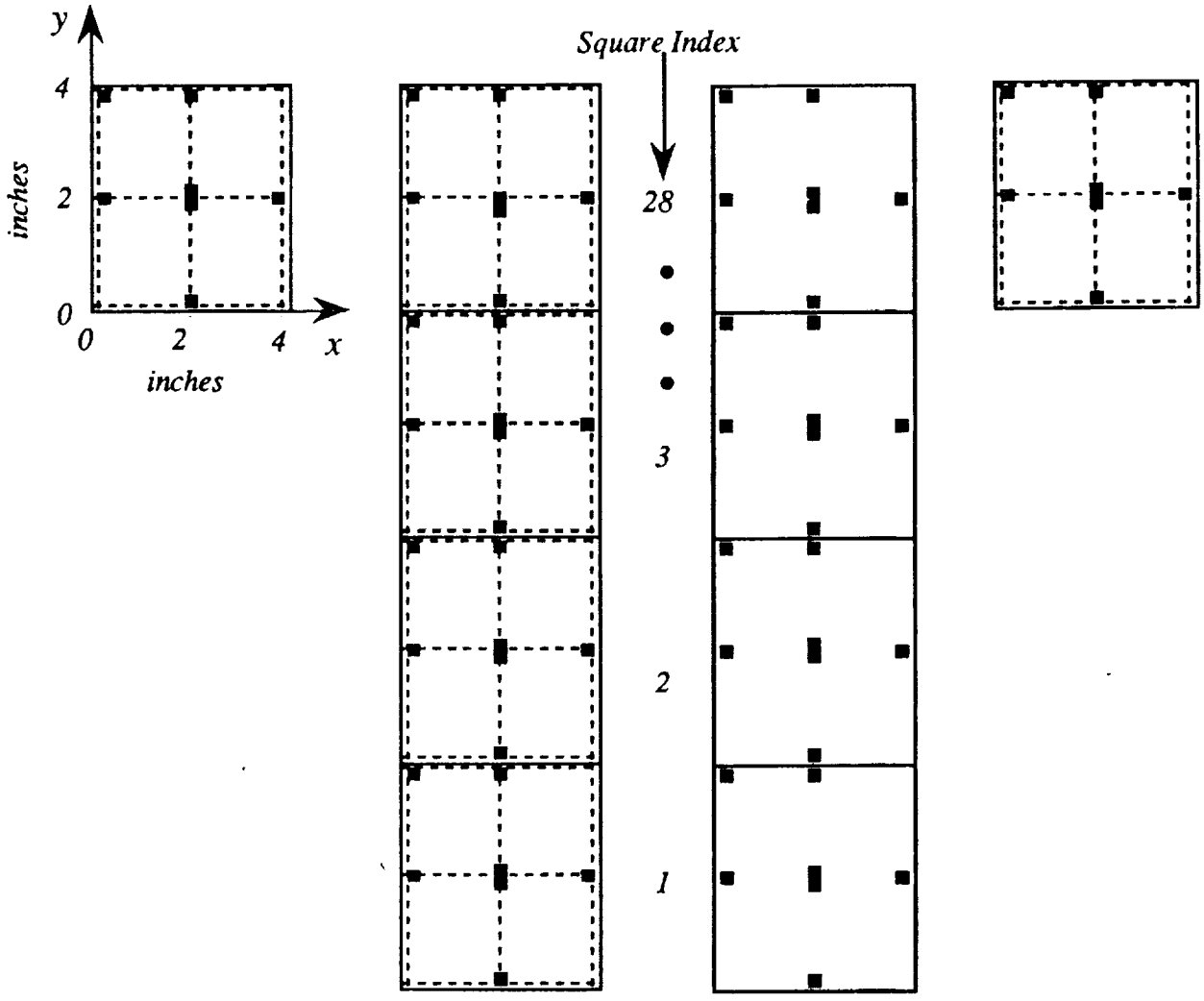

Figure 5.2 Visual calibration strip for the ARID robot.

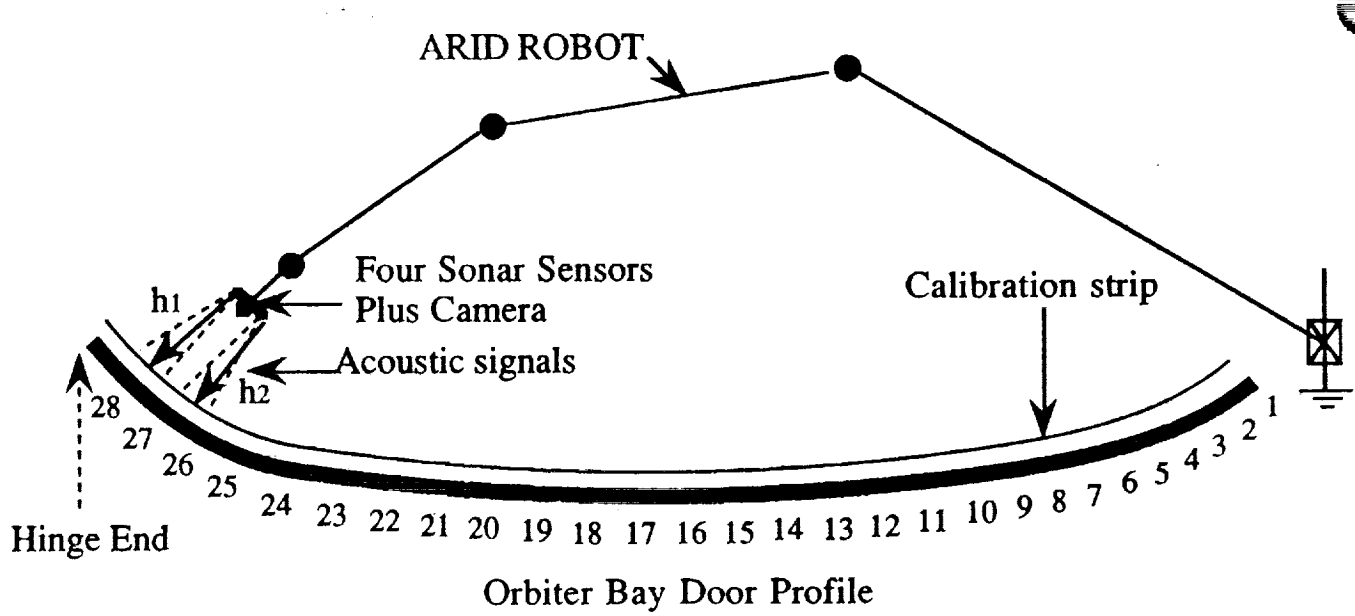

Figure 5.3 Layout of the four inch wide calibration strip. Indexes mark four inch intervals on the bay door.

5.3 Image Measurements

Figure 5.4 depicts the image frame x'-y'-z', the camera frame x-y-z, and the calibration frame x_c-y_c -z_c . The camera coordinates of an object point $\mathbf{p} = [x \;\; y \;\; z]^\tau$ on the calibration strip and its image point $\mathbf{p}' = [x' \;\; y' \;\; f\,]^\tau$ satisfy the projection equations

$$\frac{x'}{f} = \frac{x}{z} \qquad \text{and} \qquad \frac{y'}{f} = \frac{y}{z} .$$

The vision system yields the image coordinates x' and y' and the focal length f of the camera. The camera z-coordinate of the object point can be determined a number of ways. Section 7.4 derives an expression for x,y,z based upon the image data and the acoustic measurements performed by.the four sonar sensors.

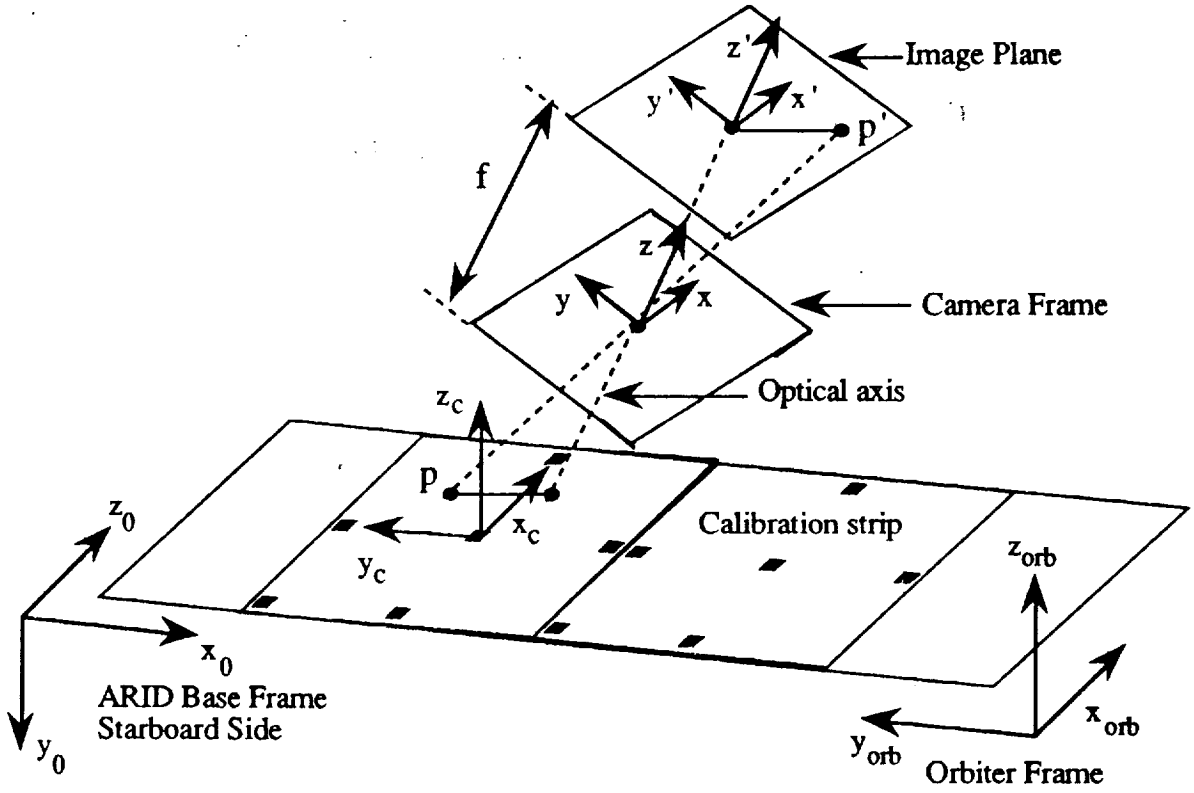

Figure 5.4 Depiction of the image, camera, calibration, ARID and Orbiter frames.

In Fig. 5.5 the camera visual field includes fiducial points p_3, p_4, p_6 of one calibration square and points p_1 and p_2 of another. The image coordinates $\mathbf{p}_i'$ of these fiducial points, along with range information from the sonars, allow us to compute their camera-coordinates $\mathbf{p}_i$ (Section 7.4). The camera field-of-view must be large enough to include at least three non-collinear fiducials in order to determine the rigid-body transformation between the camera frame and the calibration frame. For example, in Fig. 5.5 the coordinates of $\mathbf{p}_3$, $\mathbf{p}_4$ and $\mathbf{p}_6$ yield sufficient information to do that. The vectors

$$\boldsymbol{a} := [a_x \;\; a_y]^\tau = \mathbf{p}_4 - \mathbf{p}_6 \quad \text{and} \quad \boldsymbol{b} := [b_x \;\; b_y]^\tau = \mathbf{p}_4 - \mathbf{p}_3$$

define the coordinate frame axes vectors $x_c = \frac{\mathbf{a}}{|\mathbf{a}|}$ and $y_c = \frac{\mathbf{b}}{|\mathbf{b}|}$ of the calibration square with respect to the camera frame. The third axis equals the cross-product of the other two: $z_c = x_c \times y_c$ The vectors x_c, y_c, z_c should be orthogonal. Measurement error may cause $x_c^\tau y_c \neq 0$, hence, the matrix

$$^{camera}\mathbf{R}_{calibration} = [x_c \quad y_c \quad z_c],$$

Figure 5.5 Camera image of a calibration square.

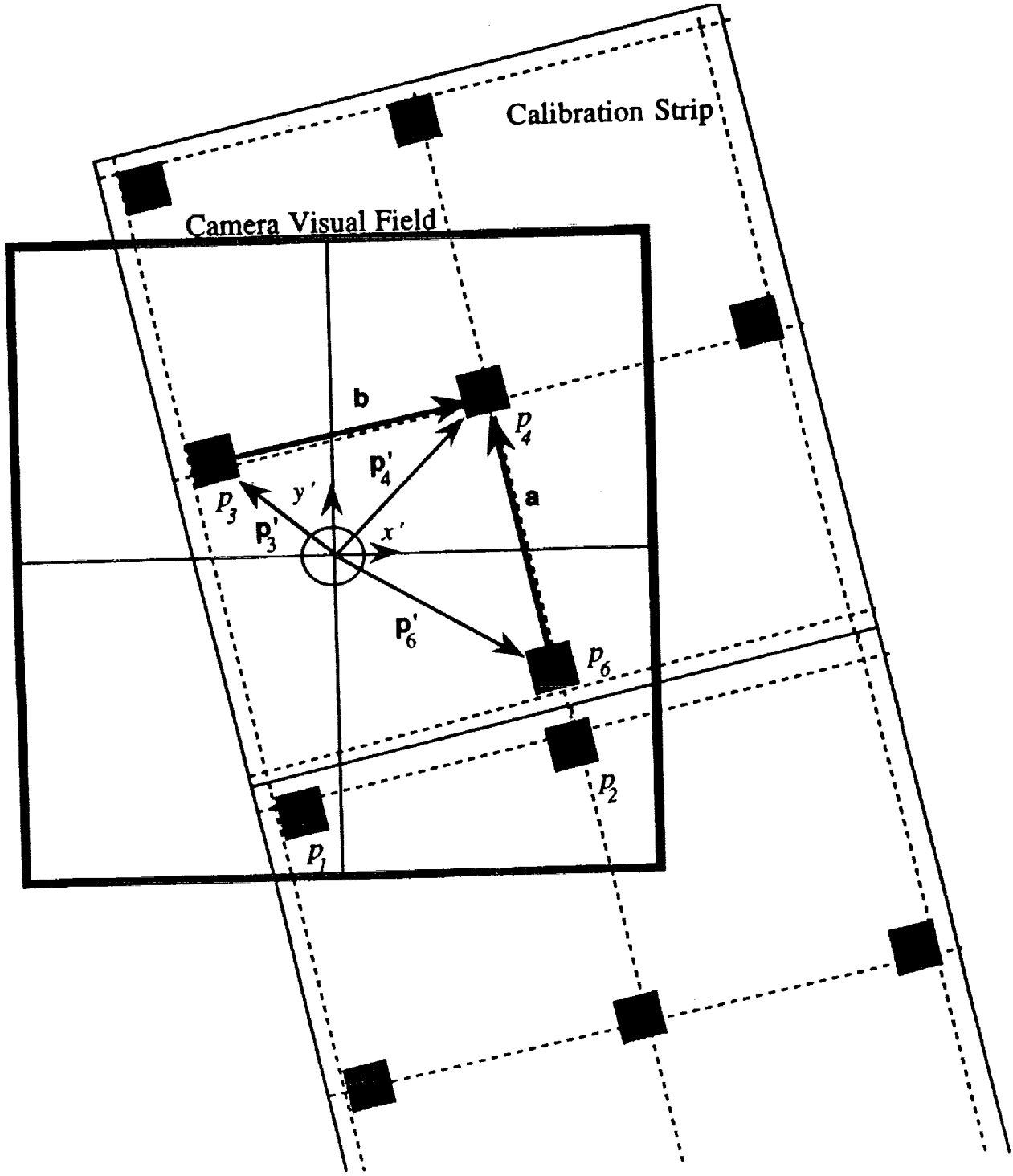

which transforms calibration-coordinates into camera-coordinates, may not be a true rotation as it would be with exact measurements. In any case, the measured rigid-body transformation which converts calibration-coordinates to camera-coordinates equals

$$ {}^{\text{camera}}\mathbf{M}_{\text{calibration}} = \begin{bmatrix} {}^{\text{camera}}\mathbf{R}_{\text{calibration}} & \mathbf{p}_4 \\ 0\ 0\ 0 & 1 \end{bmatrix}. $$

With ${}^{0}\mathbf{T}_{4}$ equal to the forward transform of the ARID and ${}^{4}\mathbf{T}_{\text{camera}}$ equal to the fixed, rigid-body transformation relating the camera-frame to the ARID end-effector frame, we have the identity,

$$ {}^{0}\mathbf{M}_{\text{calibration}} = {}^{0}\mathbf{T}_{4}\ {}^{4}\mathbf{T}_{\text{camera}}\ {}^{\text{camera}}\mathbf{M}_{\text{calibration}} $$

where ${}^{0}\mathbf{M}_{\text{calibration}}$ relates the ARID base-frame to the coordinate system of the calibration square under view. The above relationship yields one set of equations in the unknown parameters for each calibration pose measured. Section 8.0 will elaborate the procedure.

5.4 Fiducial Identification Algorithm

The above computation hinges on the assumption that the fiducial marks can be identified. Refer to Figure 5.6 in following the logic of the **FID** algorithm below. The assumption is that a center fiducial always appears in the camera field-of-view. Assume there are n pixels per inch.

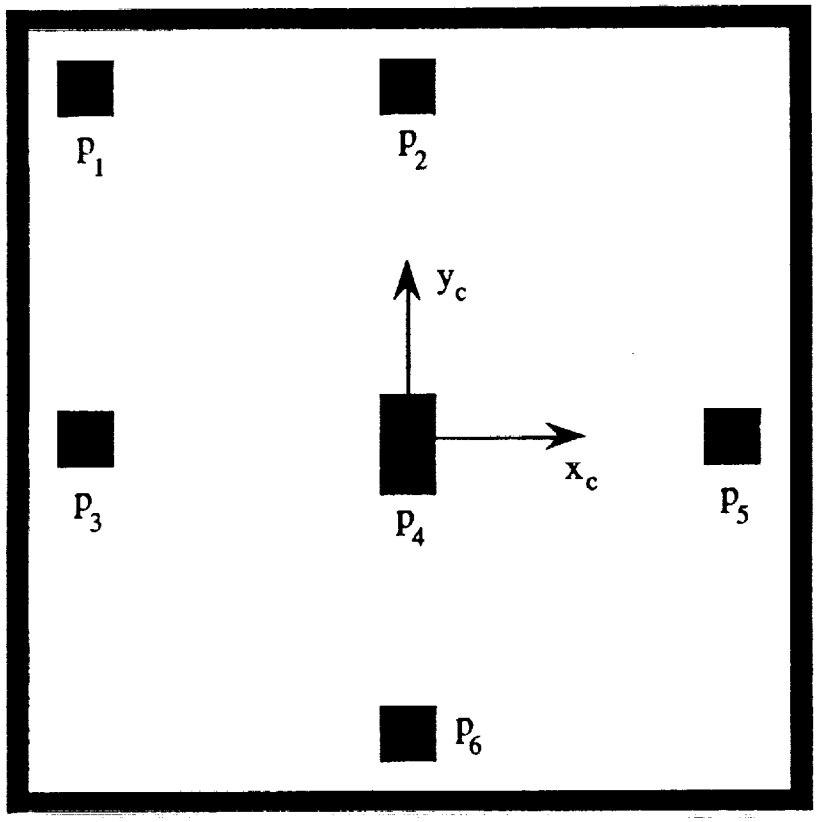

Figure 5.6 A typical calibration square with fiducial centroids indicated by p_i .

FID Algorithm

1. Scan image left-to-right, top-to-bottom, starting at the upper left-hand-corner until a blob is encountered with area: $\frac{n^2}{8}$. The centroid of that blob equals the center point $\mathbf{p}_4$. The longest side of the center blob determines the *y-axis*. The direction of the *y-axis* will usually be towards increasing *y'* of the image frame. For this not to be the case the ARID would have to be in error by 180°.

2. Determine the centroid and the midpoint of two adjacent edges of the center blob. The lines from the centroid to the two edges provide a rough estimate of the *x-* and *y-axes* of the calibration-frame in which the fiducial is located.

3. From the center fiducial search for the perimeter fiducials approximately *1.75 n* pixels along the four directions found in Step 2. Find the centroid of any blob with area equal to $\frac{n^2}{16}$ and compute the longest vector along each axis to increase the accuracy of the axes measurements.

6. ACOUSTIC MEASUREMENTS

The acoustic sensor measures four perpendicular distances h_i , $i = 1,2,3,4$, to the calibration strip (Fig. 6.1, also refer to Fig. 7.1). Section 7.0 illustrates how the acoustic measurements determine the plane of a calibration square, assuming, of course, that the bay door is locally flat. The curvature along the Orbiter's *y-axis* requires the sonar separation to be small compared to the curvature. Since we desire to calibrate the ARID every four inches, and four inches is small compared to the bay door curvature (except near the hinges), one solution would be to make the sonar separation d along the *y-axis* equal to four inches, if this is possible. The Orbiter is quite flat along the *x-axis*, so the separation of the sonar sensors can be further apart along that axis. In the ensuing discussion the distance between the two *x-axis* sonars will be assumed equal to the distance between the two *y-axis* sonars. This distance will be denoted by d.

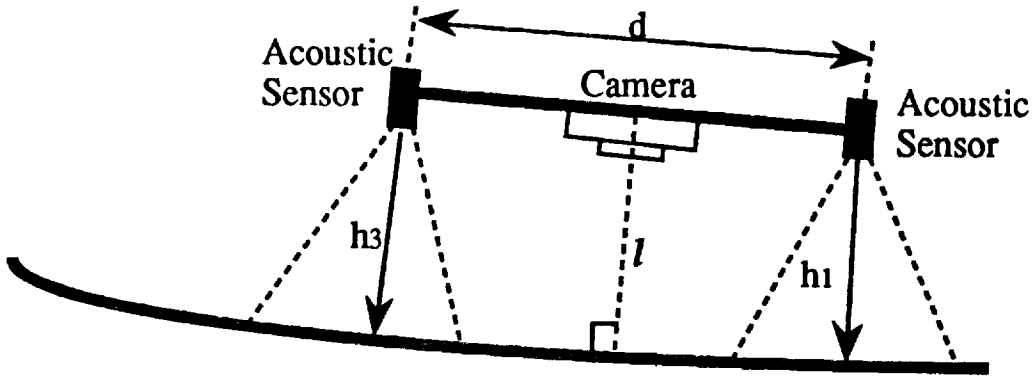

Figure 6.1 Side view of the calibration end-effector showing the camera and two of the four acoustic sensors.

We emphasize that the sonar sensors must scan a locally flat surface. Should this not be possible on an Orbiter bay door mock-up, the calibration strip can be placed on a flat surface and the ARID calibrated on that surface. From preliminary experiments with the ARID, such a calibration procedure might actually work better than using an Orbiter bay door mock-up section.

The integration of the sonar measurements with the vision imaging to locate the calibration square fiducial points in camera-frame coordinates will be described next.

7. CAMERA COORDINATES OF CALIBRATION POINTS

The goal of this section is to compute the camera-frame coordinates of the point $p = p(x,y,z)$ on the calibration strip, given

1. The absolute distance between pixels,
2. The focal length f of the camera,
2 The distance between the sonar sensors 2 γ,
3. Sonar measurements h_i , $i = 1,2,3,4$, and
4. The camera-frame coordinates of its image point $p' = p(x',y',f)$.

Figure 7.1 depicts the calibration end-effector taking a measurement. The sonar sensors measure the heights h_i , $i = 1,2,3,4$, and the camera takes an image of the calibration strip. The camera has focal length f . The distance between the sonar sensors d = 2 γ. The camera-frame origin coincides with the lens center and the optical axis coincides with the the frame's *z-axis*.

Since the fiducial points on the calibration strip have known positions, the computed coordinates of a fiducial point p can be compared to its known value, provided one can identify that fiducial. We treated the problem of identifying a specific fiducial in Section 5.4.

Measurement of the position of any three, non-collinear, fiducial points completely determines the plane of the calibration strip, the *calibration-plane*, with respect to the camera-frame and, therefore, provides a complete calibration measurement.

The acoustic measurements yield the positions of the points p_i , $i = 1,2,3,4$, on the calibration-plane. Four points over-determine the plane. Since the orbiter bay doors are not exactly flat and the acoustic measurements may not, in any case, precisely place the four points on a common plane, one may wish to find a plane that "best-fits" the four points. In this case, one may wish to employ the Moore-Penrose inverse to compute the unique plane that fits the data in a least-squares sense.

From Fig. 7.1 one can determine the camera-frame coordinates of the point p_i, $i = 1,2,3,4$, in terms of the acoustically measured heights h_i , $i = 1,2,3,4$, and the between-sensor distance d = $\sqrt{2}$ γ.

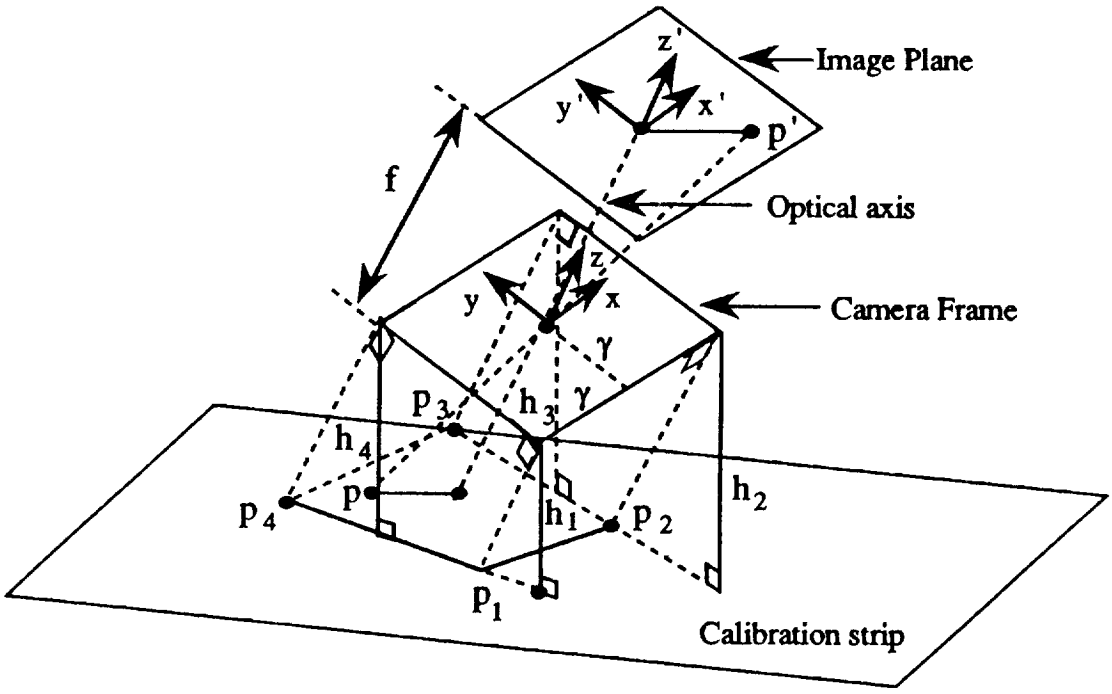

Figure 7.1 Acoustic and visual measurement parameters

Consider the detail of the plane determined by the parallel lines h_1 and h_4 in Fig. 7.2. One expects the acoustic sensor to measure the perpendicular distance to the calibration plane since the reflection along the perpendicular travels the shortest path. Experimental observation appears to verify this expectation.

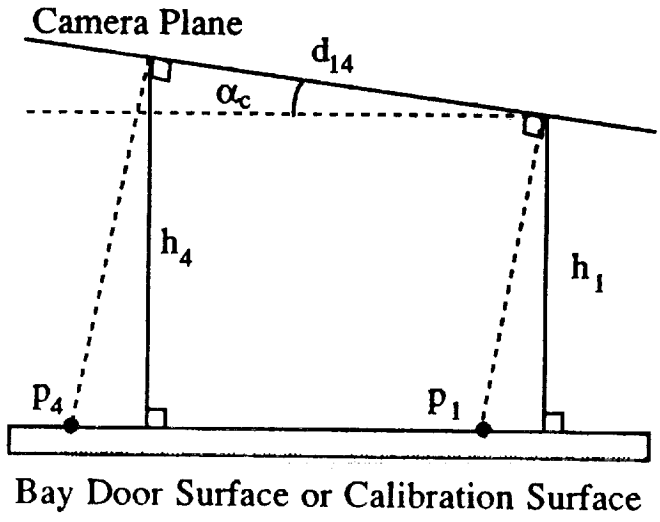

Figure 7.2 Acoustic and visual measurement parameters

The acoustic measurements h_1 and h_4 allow us to compute the camera coordinate *z-components* of the points p_1 and p_4. In Fig. 7.2, the distance $d_{14} = d\sqrt{2}$, hence,

$$\sin(\alpha_c) = \frac{h_4 - h_1}{d\sqrt{2}}. \tag{7-1}$$

The camera z-coordinates of the points p_1 and p_4 compute to

$$z_1 = \frac{-h_1}{\cos(\alpha_c)} \quad \text{and} \quad z_4 = \frac{-h_4}{\cos(\alpha_c)}, \tag{7-2}$$

hence, the camera coordinates of these two points equal, respectively,

$$\mathbf{p}_1 = \begin{bmatrix} -\gamma \\ -\gamma \\ \dfrac{-h_1}{\cos(\alpha_c)} \end{bmatrix}, \quad \mathbf{p}_4 = \begin{bmatrix} -\gamma \\ \gamma \\ \dfrac{-h_4}{\cos(\alpha_c)} \end{bmatrix}. \tag{7-3}$$

A similar consideration of the plane determined by the parallel lines h_2 and h_3 permits expressing the camera coordinates of points p_2 and p_3,

$$\mathbf{p}_2 = \begin{bmatrix} \gamma \\ -\gamma \\ \dfrac{-h_2}{\cos(\beta_c)} \end{bmatrix}, \quad \mathbf{p}_3 = \begin{bmatrix} \gamma \\ \gamma \\ \dfrac{-h_3}{\cos(\beta_c)} \end{bmatrix}. \tag{7-4}$$

In this case, the angle β_c is determined by

$$\sin(\beta_c) = \frac{h_3 - h_2}{d\sqrt{2}}. \tag{7-5}$$

These values assumes the sonar measurements determine the perpendicular distance to the calibration strip.

7.1 Computing the Calibration-Plane Equation

From the coordinates of any three of the four points p_i , $i = 1,2,3,4$, one can compute the coefficients $\{\eta_x , \eta_y , \eta_z , \xi\}$ in the calibration-plane equation,

$$\eta_x x + \eta_y y + \eta_z z + \xi = 0, \tag{7-6}$$

or, equivalently,

$$\frac{\eta_x}{\xi} x + \frac{\eta_y}{\xi} y + \frac{\eta_z}{\xi} z = -1. \tag{7-7}$$

Substituting the coordinates of p_i , $i = 1,2,3$, into the above equation leads to the linear system in the unknown coefficients,

$$\mathbf{A}\,\nu = -\begin{bmatrix} 1 \\ 1 \\ 1 \end{bmatrix}, \tag{7-8}$$

where

$$\mathbf{A} = \begin{bmatrix} -\gamma & -\gamma & \dfrac{-h_1}{\cos(\alpha_c)} \\ \gamma & -\gamma & \dfrac{-h_2}{\cos(\beta_c)} \\ \gamma & \gamma & \dfrac{-h_3}{\cos(\beta_c)} \end{bmatrix}, \qquad \nu = \begin{bmatrix} \nu_x \\ \nu_y \\ \nu_z \end{bmatrix} = \frac{1}{\xi}\begin{bmatrix} \eta_x \\ \eta_y \\ \eta_z \end{bmatrix}. \tag{7-9}$$

As long as p_i , $i = 1,2,3$, are not collinear, **A** is invertible and

$$\nu = -\mathbf{A}^{-1}\begin{bmatrix} 1 \\ 1 \\ 1 \end{bmatrix}, \tag{7-10}$$

determines the coefficients for the plane equation.

This method can be applied to all four points as well, except that **A** becomes $\mathbf{A} = [\mathbf{p}_1 \ \mathbf{p}_2 \ \mathbf{p}_3 \ \mathbf{p}_4]^\tau$, and is no longer invertible. The Moore-Penrose inverse (pseudo-inverse) $\mathbf{A}^+$, however, can be used to find a plane that fits the data in a least-squares sense. The resultant solution ν_s computes to

$$\nu_s = -\mathbf{A}^+ \begin{bmatrix} 1 \\ 1 \\ 1 \end{bmatrix}. \tag{7-11}$$

If three of the four points are not colinear, **A** has full-column rank and

$$\mathbf{A}^+ = (\mathbf{A}^\tau \mathbf{A})^{-1} \mathbf{A}^\tau . \tag{7-12}$$

The solution obtained with the Moore-Penrose inverse yields a plane equation that fits the data with least-squared-error ε,

$$\varepsilon := \left| -\begin{bmatrix} 1 \\ 1 \\ 1 \end{bmatrix} - \mathbf{A}\,\nu_s \right|^2 \leq \left| -\begin{bmatrix} 1 \\ 1 \\ 1 \end{bmatrix} - \mathbf{A}\,\nu \right|^2 \quad \text{for all } \nu. \tag{7-13}$$

In other words, no other plane will produce a smaller ε than the plane determined by the coefficients ν_s.

7.2 Alternative Computation of the Calibration-Plane Equation

The computation of the coefficients of the calibration-plane equation in the previous discussion required the inversion of the matrix **A**. The computational requirements are significantly reduced and symbolic solutions obtained by taking advantage of the properties of a plane.

From the coordinates of three, non-collinear points p_i , $i = 1,2,3$, compute the coefficients in the calibration-plane equation,

$$\eta_x x + \eta_y y + \eta_z z + \xi = 0, \tag{7-14}$$

by computing the coefficients of x,y, and z in

$$[x \ \ y \ \ z] \cdot (\mathbf{p}_2 - \mathbf{p}_1) \times (\mathbf{p}_3 - \mathbf{p}_1) + \xi = 0. \tag{7-15}$$

and the constant term from

$$\xi = -\mathbf{p}_1^{\tau}(\mathbf{p}_2-\mathbf{p}_1)\times(\mathbf{p}_3-\mathbf{p}_1)\,. \tag{7-16}$$

The first term in the above equation is the vector box product, hence, the coefficients may also be computed in terms of determinants. For the situation depicted in Fig. 7.1, for example,

$$[x \quad y \quad z\,]\cdot(\mathbf{p}_2-\mathbf{p}_1)\times(\mathbf{p}_3-\mathbf{p}_1) = \begin{vmatrix} x & y & z \\ 2\gamma & 0 & \frac{h_1}{\cos(\alpha_c)} - \frac{h_2}{\cos(\beta_c)} \\ 2\gamma & 2\gamma & \frac{h_1}{\cos(\alpha_c)} - \frac{h_3}{\cos(\beta_c)} \end{vmatrix}. \tag{7-17}$$

The coefficients of x,y,z in the resulting express for the above determinant equal

$$\eta_x = 2\gamma\left(\frac{h_2}{\cos(\beta_c)} - \frac{h_1}{\cos(\alpha_c)}\right), \quad \eta_y = 2\gamma\frac{h_3-h_2}{\cos(\beta_c)}, \quad \eta_z = 4\gamma^2. \tag{7-18}$$

To calculate the constant ξ evaluate

$$\xi = -\begin{vmatrix} -\gamma & -\gamma & \frac{-h_1}{\cos(\alpha_c)} \\ 2\gamma & 0 & \frac{h_1}{\cos(\alpha_c)} - \frac{h_2}{\cos(\beta_c)} \\ 2\gamma & 2\gamma & \frac{h_1}{\cos(\alpha_c)} - \frac{h_3}{\cos(\beta_c)} \end{vmatrix} = -\begin{vmatrix} -\gamma & -\gamma & \frac{-h_1}{\cos(\alpha_c)} \\ 2\gamma & 0 & \frac{h_1}{\cos(\alpha_c)} - \frac{h_2}{\cos(\beta_c)} \\ 0 & 0 & \frac{-h_1}{\cos(\alpha_c)} - \frac{h_3}{\cos(\beta_c)} \end{vmatrix} \tag{7-19}$$

to obtain

$$\xi = 2\gamma^2\left(\frac{h_1}{\cos(\alpha_c)} + \frac{h_3}{\cos(\beta_c)}\right). \tag{7-20}$$

Collecting these results together yields,

$$\nu_1 = \frac{1}{\gamma\left(\frac{h_1}{\cos(\alpha_c)} + \frac{h_3}{\cos(\beta_c)}\right)} \begin{bmatrix} \left(\frac{h_2}{\cos(\beta_c)} - \frac{h_1}{\cos(\alpha_c)}\right) \\ \frac{h_3 - h_2}{\cos(\beta_c)} \\ 2\gamma \end{bmatrix}. \qquad (7\text{-}21)$$

If the three points p_i , $i = 1,2,4,$ had been selected to determine the plane, then

$$\nu_2 = \frac{1}{\gamma\left(\frac{h_2}{\cos(\beta_c)} + \frac{h_4}{\cos(\alpha_c)}\right)} \begin{bmatrix} \frac{h_2}{\cos(\beta_c)} - \frac{h_1}{\cos(\alpha_c)} \\ \frac{h_4 - h_1}{\cos(\alpha_c)} \\ 2\gamma \end{bmatrix} \qquad (7\text{-}22)$$

and $$\xi = 2\gamma^2\left(\frac{h_2}{\cos(\beta_c)} + \frac{h_4}{\cos(\alpha_c)}\right). \qquad (7\text{-}23)$$

A necessary and sufficient condition for the two sets of plane coefficients to be the same, $\nu_1 = \nu_2$, is that

$$\frac{h_1}{\cos(\alpha_c)} + \frac{h_3}{\cos(\beta_c)} = \frac{h_2}{\cos(\beta_c)} + \frac{h_4}{\cos(\alpha_c)} . \qquad (7\text{-}24)$$

If the measured heights satisfy this condition, then all four points must be on the same plane. Of course, with measurements, one cannot guarantee this condition will hold and the more complex, least-squared solution may be preferred.

Now that we have the equation for the calibration-plane, we can use the visual data to compute the camera-coordinates of any point p on the calibration-plane from the coordinates of its image point p' on the image plane.

7.3 Camera-Coordinates of a Point on the Calibration Strip

From geometric optics and the coordinate frame definitions depicted in Fig. 7.1, the coordinates of $\mathbf{p} = [x \quad y \quad z]^\tau$ and its image point $\mathbf{p}' = [x' \quad y' \quad f\,]^\tau$ satisfy the projection equations

$$\frac{x'}{f} = \frac{x}{z} \quad \text{and} \quad \frac{y'}{f} = \frac{y}{z} . \qquad (7\text{-}25)$$

In Fig. 7.1 the *z-axis* component of the object must always be negative.

Since every point p on the calibration-plane must satisfy

$$\nu^{\tau} \mathbf{p} = -1, \tag{7-26}$$

one can compute the range of the object in terms of its x and y coordinates,

$$z = \frac{\nu_x x + \nu_y y + 1}{-\nu_z}. \tag{7-27}$$

Substitute into (7-27) the values for x and y given in (7-25) and solve for z to obtain

$$z = \frac{-f}{\nu_x x' + \nu_y y' + \nu_z f}. \tag{7-28}$$

Computing x and y with this value of z yields

$$\begin{bmatrix} x \\ y \end{bmatrix} = \frac{-1}{\nu_x x' + \nu_y y' + \nu_z f} \begin{bmatrix} x' \\ y' \end{bmatrix}. \tag{7-29}$$

From ν_1 computed earlier (7-21) and the definitions

$$\eta_1 := \frac{h_1}{\cos(\alpha_c)}, \quad \eta_2 := \frac{h_2}{\cos(\beta_c)}, \quad \eta_3 := \frac{h_3}{\cos(\beta_c)}, \quad \eta_4 := \frac{h_4}{\cos(\alpha_c)}, \tag{7-30}$$

$$\cos(\alpha_c) = \sqrt{1 - \left(\frac{h_4 - h_1}{d\sqrt{2}}\right)^2},$$

and

$$\cos(\beta_c) = \sqrt{1 - \left(\frac{h_3 - h_2}{d\sqrt{2}}\right)^2},$$

we obtain the camera coordinates x, y of any point in the object plane in terms of the acoustic measurements h_i, the visual measurements x', y', and the distance d between the sonar sensors,

$$\begin{bmatrix} x \\ y \end{bmatrix} = \frac{-\gamma(\eta_1 + \eta_3)}{(\eta_2 - \eta_1) x' + (\eta_3 - \eta_2) y' + 2\gamma f} \begin{bmatrix} x' \\ y' \end{bmatrix} \tag{7-31}$$

and

$$z = \frac{-\gamma f (\eta_1 + \eta_3)}{(\eta_2 - \eta_1) x' + (\eta_3 - \eta_2) y' + 2 \gamma f}. \qquad (7\text{-}32)$$

In the next section the camera coordinates of the fiducial points will be used to determine the rigid-body transformation between the camera and calibration square under view.

7.4 The Camera-to-Calibration-Frame Transformation

Assume the fiducial centroids p_i , $i = 1,2,3,4,5$, on a calibration square have been identified (Fig. 7.3) by the ***FID*** algorithm. In Section 7.3 we indicated how the camera coordinates x_i ,y_i , z_i of each fiducial centroid p_i can be calculated from acoustic measurements and the camera image-coordinates x_i', y_i' of its image point p_i'. Therefore, the camera-frame coordinates of the calibration-frame of the square under view equal

$$\mathbf{x}_c = \frac{\mathbf{p}_5 - \mathbf{p}_3}{|\mathbf{p}_5 - \mathbf{p}_3|}, \quad \mathbf{y}_c = \frac{\mathbf{p}_2 - \mathbf{p}_6}{|\mathbf{p}_2 - \mathbf{p}_6|}, \quad \mathbf{z}_c = \mathbf{x}_c \times \mathbf{y}_c . \qquad (7\text{-}33)$$

These vectors should be orthogonal. Measurement error may cause $\mathbf{x}_c^{\tau}\, \mathbf{y}_c \neq 0$, hence, the matrix

$$^{\text{camera}}\mathbf{R}_{\text{calibration}} = [\mathbf{x}_c \quad \mathbf{y}_c \quad \mathbf{z}_c], \qquad (7\text{-}34)$$

which transforms calibration-coordinates into camera-coordinates may not be a true rotation as it would be with exact measurements. In any case, the measured rigid-body transformation which converts calibration-coordinates to camera-coordinates equals

$$^{\text{camera}}\mathbf{M}_{\text{calibration}} := \begin{bmatrix} ^{\text{camera}}\mathbf{R}_{\text{calibration}} & \mathbf{p}_4 \\ 0\ 0\ 0 & 1 \end{bmatrix}. \qquad (7\text{-}35)$$

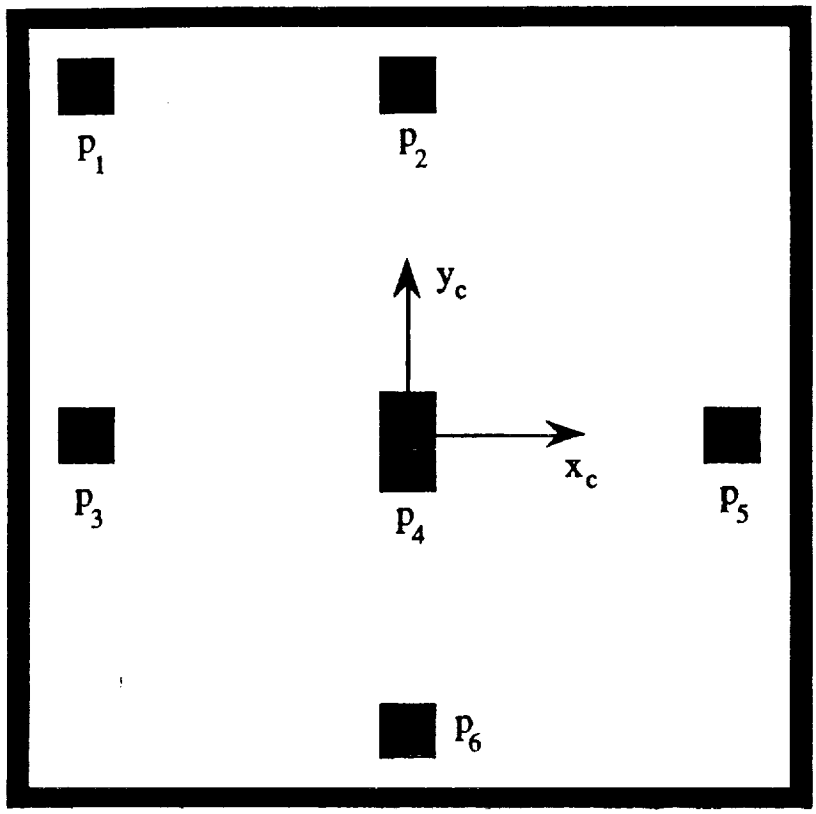

Figure 7.3 A typical calibration square with fiducial centroids indicated by p_i.

Knowledge of the ARID forward kinematics, the relationship of the camera-frame to the ARID end-frame and, now, the camera-coordinates of the fiducial points, one can compute the fiducial point coordinates with respect to the ARID base frame. Assuming the calibration strip has been accurately positioned with respect to the ARID base frame, one can consequently calibrate the ARID at each calibration square by comparing the calibrated, fiducial-point, base-frame coordinates with the measured fiducial-point, base-frame coordinates. In the next section, these ideas will be developed further.

8. CALIBRATION OF THE ARID

Let ${}^{0rb}\mathbf{M}_{calibration}$ be a precisely measured rigid-body transformation from the Orbiter frame to a calibration square of interest. Define ${}^{0rb}\mathbf{M}_0$ to be a precisely measured rigid-body transformation from the Orbiter frame to the ARID base-frame. The rigid-body transformation ${}^{4}\mathbf{M}_{camera}$, relating the camera frame to the ARID end-frame is fixed and assumed known. If this is not the case, a tool-frame calibration-model must be appended to the existing ARID model and additional

kinematic parameters will need to be determined along with the ARID parameters. To simplify the development here, ${}^{4}\mathbf{M}_{camera}$ is assumed known. The rigid-body transformation ${}^{camera}\mathbf{M}_{calibration}$ (7-35) is calculated from the acoustic and visual measurements.

The rigid-body transformation from the Orbiter frame to the calibration-frame must equal

$$ {}^{0rb}\mathbf{M}_{calibration} = {}^{0rb}\mathbf{M}_{0}\ {}^{0}\mathbf{T}_{4}\ {}^{4}\mathbf{M}_{camera}\ {}^{camera}\mathbf{M}_{calibration} \qquad (7\text{-}35) $$

Solving for ${}^{0}\mathbf{T}_{4}$ yields

$$ {}^{0}\mathbf{T}_{4} = {}^{0}\mathbf{M}_{0rb}\ {}^{0rb}\mathbf{M}_{calibration}\ {}^{calibration}\mathbf{M}_{camera}\ {}^{camera}\mathbf{M}_{4} \qquad (7\text{-}35) $$

All the transformations on the left-side of (7-35) are known. If we assume the joint displacements are accurately known then one can solve for the unknown kinematic parameters in ${}^{0}\mathbf{T}_{4}$ (3-10), namely, a_i, $i = 1,2,3$, and the eight angle parameters in ψ (3-12). Since (7-35) only provides 7 equations, two independent measurements will be required.

From the two measurements eight equations and eight unknowns derive from (3-11a,b,c,d). If the resulting 8×8 matrix is well conditioned, then it may be inverted to compute ψ , independently of the linear parameters a_i . In this approach (3-11e) could serve as a partial check of the solution.

For the ARID, the three linear parameters a_i can be solved by a set of equations based on the first two entries of the last column of ${}^{0}\mathbf{T}_{4}$. These equations, interestingly, do not depend upon the angle parameters in ψ to first order.

9. CONCLUSIONS

A kinematics error-model and an experimental procedure has been proposed for calibrating the ARID robot. A camera and sonar end-effector measures the pose of the ARID end-frame for different calibration poses. A minimum of two measurements determine the kinematics calibration-model of the ARID for a particular calibration-square, assuming the joint displacements are accurately measured, the calibration surface is planar, and the kinematic parameters do not vary rapidly in the region above a particular four inch calibration square. Preliminary experiments suggest this is the case.

Recommendations

The theoretical developments presented in this paper and the experimental results expressed in a companion paper [1], suggest that the ARID manipulator will admit of effective calibration. On this basis the author encourages the Robotics Section to vigorously pursue implementation of the calibration technique described herein.

REFERENCES

[1] Doty, K.L., 1992, "Arid Relative Calibration Experimental Data and Analysis", NASA Faculty Fellow Report, Kennedy Space Center.

[2] Horn, B.K.P., 1986, *Robot Vision*, MIT Press, Cambridge Mass.